October 17, 2018

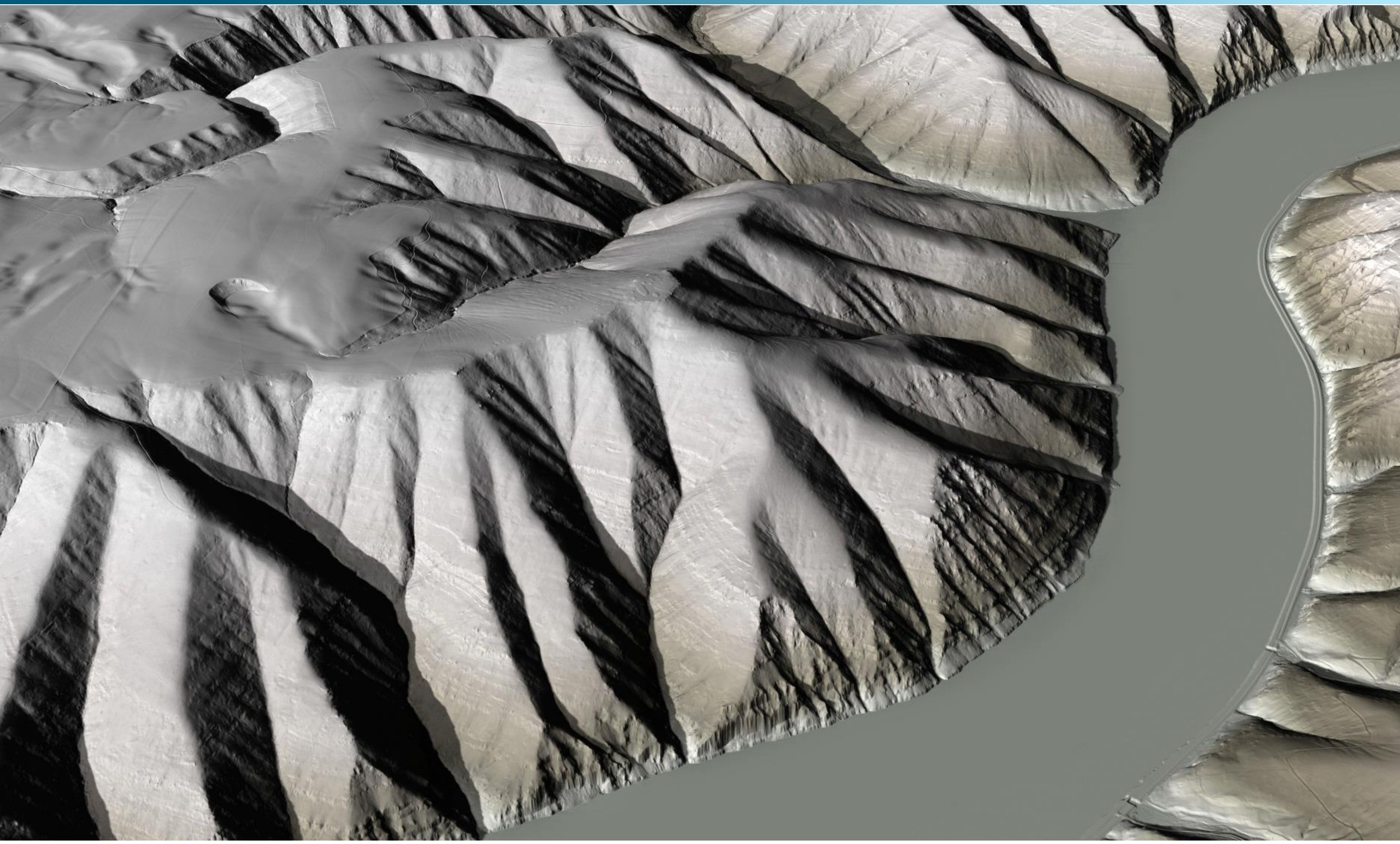

Washington 3 Counties LiDAR Technical Data Report, Contract G16PC00016, Task Order G17PD01222

Revised January 2019

Prepared For:

USGS
science for a changing world

Amanda Lowe
USGS NGTOC
1400 Independence Rd. MS547
Rolla, MO 65401
PH: 573-308-3500

Prepared By:

quantum SPATIAL

QSI Corvallis
1100 NE Circle Blvd, Ste. 126
Corvallis, OR 97330
PH: 541-752-1204

Table of Contents

Introduction ... 1
Deliverable Products ... 2
Acquisition ... 4
Planning ... 4
Airborne Survey ... 5
LiDAR ... 5
Ground Control ... 7
Base Stations ... 7
Ground Survey Points (GSPs) ... 9
Land Cover Class ... 10
Processing ... 13
LiDAR Data ... 13
Temporal Snow Classification ... 14
Feature Extraction ... 15
Hydro-flattening and Water's Edge Breaklines ... 15
Results & Discussion ... 16
LiDAR Density ... 16
LiDAR Accuracy Assessments ... 23
LiDAR Non-Vegetated Vertical Accuracy ... 23
LiDAR Vegetated Vertical Accuracy ... 26
LiDAR Relative Vertical Accuracy ... 27
Certifications ... 28
Selected Images ... 29
Glossary ... 31
Appendix A - Accuracy Controls ... 32

Cover Photo: A view overlooking the Snake River and its surrounding terrain on the edge of the Washington 3 Counties AOI. The image was created from the LiDAR bare earth model colored by elevation.

INTRODUCTION

This photo taken by QSI acquisition staff shows a view of the rugged southwestern region inside the Washington 3 Counties AOI.

In September 2017, Quantum Spatial (QSI) was contracted by the United States Geological Survey (USGS) to collect Light Detection and Ranging (LiDAR) data in the fall and winter of 2017, and spring of 2018 for the Washington 3 Counties site. The Washington 3 Counties project area encompasses approximately 1.85 million acres spread out over the Columbia, Garfield, and Walla Walla counties. Data were collected to aid USGS in assessing the topographic and geophysical properties of the study area and to add to the 3DEP national database.

This report accompanies the delivered LiDAR data and documents contract specifications, data acquisition procedures, processing methods, and analysis of the final dataset including LiDAR accuracy and density. Acquisition dates and acreage are shown in Table 1, a complete list of contracted deliverables provided to USGS is shown in Table 2, and the project extent is shown in Figure 1.

Table 1: Acquisition dates, acreage, and data types collected on the Washington 3 Counties site

Project Site	Contracted Acres	Buffered Acres	Acquisition Dates	Data Type
Washington 3 Counties – QL1 AOI	968,840	973,639	11/10/17, 11/12/17, 11/15/17, 02/10/18 – 02/13/18, 02/20/18, 03/20/18, 03/23/18, 03/25/18, 03/26/18, 03/31/18, 04/01/18, 04/11/18, 04/21/18 – 04/24/18, 04/26/18, 04/27/18, 05/01/18 – 05/05/18, 07/04/18	QL 1 LiDAR

Project Site	Contracted Acres	Buffered Acres	Acquisition Dates	Data Type
Washington 3 Counties – QL2 AOI	887,486	893,465	10/03/17 – 10/06/17, 11/10/17, 11/11/17, 11/14/17, 11/18/17, 11/19/17, 02/10/18, 02/11/18, 03/19/18, 03/20/18	QL 2 LiDAR

Deliverable Products

Table 2: Products delivered to USGS for the Washington 3 Counties sites

Washington 3 Counties LiDAR Products Projection: Washington State Plane South Horizontal Datum: NAD83 (2011) Vertical Datum: NAVD88 (GEOID12B) Units: US Survey Feet	
Points	LAS v 1.4 • All Classified Returns • Raw Unclassified Flightline Swaths
Rasters	3 Foot ESRI Grids • Hydroflattened Bare Earth Digital Elevation Model (DEM) • Highest Hit Digital Surface Model (DSM) 3.0 Foot GeoTiffs • Intensity Images
Vectors	Index Shapefiles (*.shp) • Site Boundary • Tile Index • Breaklines • Flightline Trajectories • Snow Classification Polygon Ground Survey Shapefiles (*.shp) • Non-Vegetated Ground Check Points • Vegetated Ground Check Points • Ground Control Points • Ground Control Monuments & CORS Stations

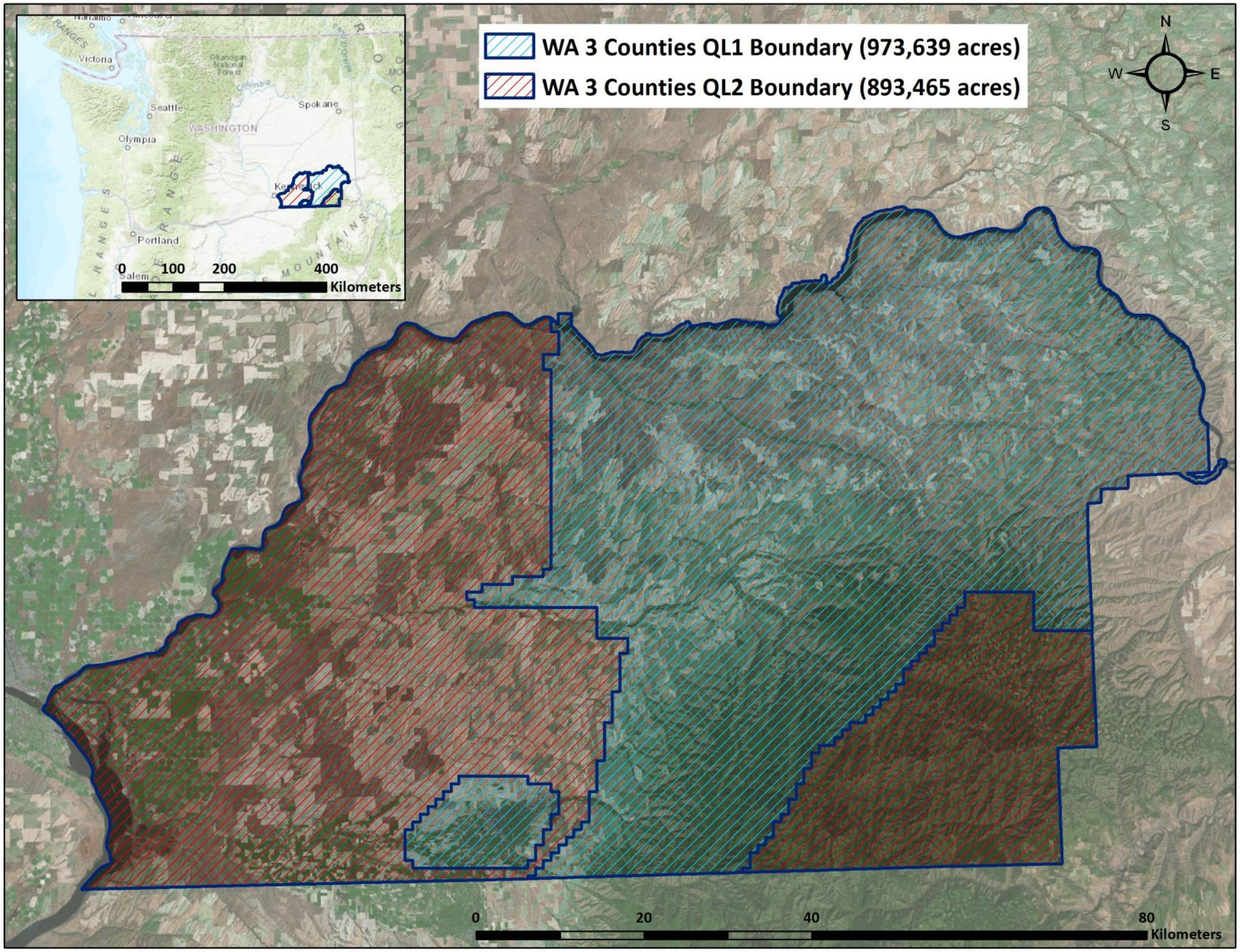

Figure 1: Location map of the Washington 3 Counties site in Washington

QSI's ground acquisition equipment set up over monument WALLA_05 in the Washington 3 Counties LiDAR study area.

Planning

In preparation for data collection, QSI reviewed the project area and developed a specialized flight plan to ensure complete coverage of the Washington 3 Counties LiDAR study area at the target point density of ≥8 points/m^2 (0.74 points/ft^2) for QL1 AOIs and ≥2 points/m^2 (0.19 points/ft^2) for QL2 AOIs. Acquisition parameters including orientation relative to terrain, flight altitude, pulse rate, scan angle, and ground speed were adapted to optimize flight paths and flight times while meeting all contract specifications.

Factors such as satellite constellation availability and weather windows must be considered during the planning stage. Any weather hazards or conditions affecting the flights were continuously monitored due to their potential impact on the daily success of airborne and ground operations. In addition, logistical considerations including private property access and potential air space restrictions were reviewed.

Airborne Survey

LiDAR

The LiDAR survey was accomplished using a Leica ALS80 system mounted in a Cessna Caravan. Table 3 summarizes the settings used to yield an average pulse density of ≥8 points/m^2 (0.74 points/ft^2) for QL1 AOIs and ≥2 points/m^2 (0.19 points/ft^2) for QL2 AOIs in the Washington 3 Counties project area. The Leica ALS80 laser system can record unlimited range measurements (returns) per pulse. It is not uncommon for some types of surfaces (e.g., dense vegetation or water) to return fewer pulses to the LiDAR sensor than the laser originally emitted. The discrepancy between first return and overall delivered density will vary depending on terrain, land cover, and the prevalence of water bodies. All discernible laser returns were processed for the output dataset.

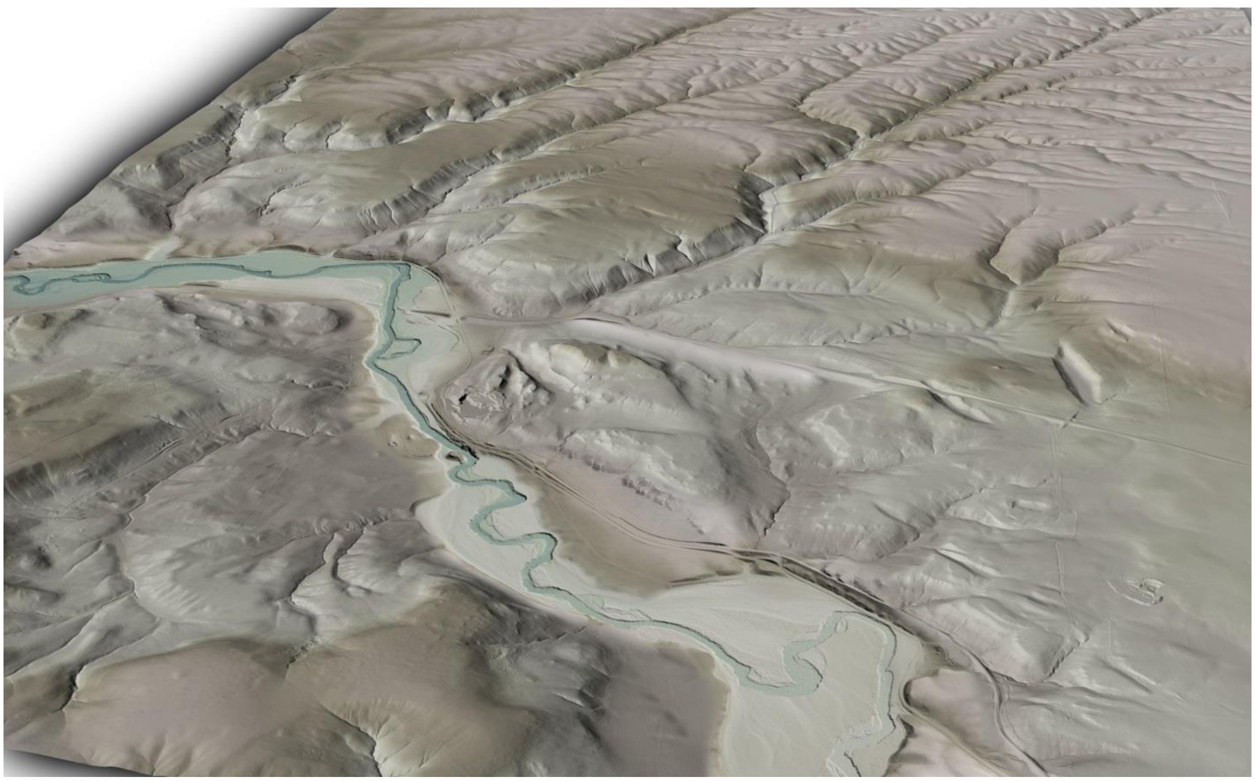

A view overlooking the Walla Walla River inside the Washington 3 Counties AOI. The image was created from the LiDAR bare earth model colored by elevation.

Table 3: LiDAR specifications and survey settings

LiDAR Survey Settings & Specifications		
AOI	QL1	QL2
Acquisition Dates	11/10/17, 11/12/17, 11/15/17, 02/10/18 – 02/13/18, 02/20/18, 03/20/18, 03/23/18, 03/25/18, 03/26/18, 03/31/18, 04/01/18, 04/11/18, 04/21/18 – 04/24/18, 04/26/18, 04/27/18, 05/01/18 – 05/05/18, 07/04/18	10/03/17 – 10/06/17, 11/10/17, 11/11/17, 11/14/17, 11/18/17, 11/19/17, 02/10/18, 02/11/18, 03/19/18, 03/20/18
Aircraft Used	Cessna Caravan 208B	
Sensor	Leica	
Laser	ALS80	
Maximum Returns	Unlimited	
Resolution/Density	Average 8 pulses/m^2	Average 2 pulses/m^2
Nominal Pulse Spacing	0.35	0.70
Survey Altitude (AGL)	1650 m	2100 m
Survey speed	145 knots	
Field of View	30º	40º
Mirror Scan Rate	48 Hz	88 Hz
Target Pulse Rate	335 kHz	250 kHz
Pulse Duration	2.5 ns	
Pulse Width	75 cm	
Central Wavelength	1064 nm	
Pulse Mode	Multiple Pulse in Air (MPiA)	
Beam Divergence	0.22 mrad	
Swath Width	884 m	1529 m
Swath Overlap	67%	63%
Intensity	16-bit	
Accuracy	$RMSE_Z$ (Non-Vegetated) ≤ 10 cm	
	NVA (95% Confidence Level) ≤ 19.6 cm	
	VVA (95^{th} Percentile) ≤ 30cm	

All areas were surveyed with an opposing flight line side-lap of ≥50% (≥100% overlap) in order to reduce laser shadowing and increase surface laser painting. To accurately solve for laser point position (geographic coordinates x, y and z), the positional coordinates of the airborne sensor and the attitude of the aircraft were recorded continuously throughout the LiDAR data collection mission. Position of the aircraft was measured twice per second (2 Hz) by an onboard differential GPS unit, and aircraft attitude was measured 200 times per second (200 Hz) as pitch, roll and yaw (heading) from an onboard inertial measurement unit (IMU). To allow for post-processing correction and calibration, aircraft and sensor position and attitude data are indexed by GPS time.

Ground Control

Ground control surveys, including monumentation and ground survey points (GSPs) were conducted to support the airborne acquisition. Ground control data were used to geospatially correct the aircraft positional coordinate data and to perform quality assurance checks on the final LiDAR dataset.

QSI's professional land surveyor, Evon Silvia (WAPLS#53957) oversaw and certified the ground survey.

Base Stations

The spatial configuration of base stations provided redundant control within 13 nautical miles of the mission areas for LiDAR flights. Base stations were also used for collection of ground survey points using real time kinematic (RTK), post processed kinematic (PPK), and fast static (FS) survey techniques. Base station locations were selected with consideration for satellite visibility, field crew safety, and optimal location for GSP coverage.

QSI utilized 3 existing NGS monuments, 8 existing non-NGS monuments, and established 7 new monuments for the Washington 3 Counties LiDAR project (Table 4, Figure 2). New monumentation was set using 5/8" x 30" rebar topped with stamped 2 ½ " aluminum caps.

Monuments were established according to the national standard for geodetic control networks, as specified in the Federal Geographic Data Committee (FGDC) Geospatial Positioning Accuracy Standards for geodetic networks.[1] This standard provides guidelines for classification of monument quality at the 95% confidence interval as a basis for comparing the quality of one control network to another. The monument rating for this project is shown in Table 5.

For the Washington 3 Counties LiDAR project, the monument coordinates contributed no more than 2.8 cm of positional error to the geolocation of the final ground survey points and LiDAR, with 95% confidence.

In addition, QSI utilized 11 permanent static GNSS stations from two networks as base stations for kinematic processing and GSP collection: 7 stations from the Washington State Reference Network (WSRN) and 4 stations from the Leica SmartNet Real-time Network. See Table 6 for a full listing of permanent base stations.

To correct the continuously recorded onboard measurements of the aircraft position, QSI utilized multiple static Global Navigation Satellite System (GNSS) ground survey sessions (1 Hz recording frequency) from each base station location. During post-processing, the static GNSS data were triangulated with nearby Continuously Operating Reference Stations (CORS) using the Online Positioning User Service (OPUS[2]) for precise positioning. Multiple independent sessions over the same location were processed to confirm antenna height measurements and to refine position accuracy.

[1] Federal Geographic Data Committee, Geospatial Positioning Accuracy Standards (FGDC-STD-007.2-1998). Part 2: Standards for Geodetic Networks, Table 2.1, page 2-3. http://www.fgdc.gov/standards/projects/FGDC-standards-projects/accuracy/part2/chapter2

[2] OPUS is a free service provided by the National Geodetic Survey to process corrected monument positions. http://www.ngs.noaa.gov/OPUS.

Table 4: Monuments utilized for the Washington 3 Counties acquisition. Coordinates are on the NAD83 (CORS96) datum, epoch 2002.00

Monument ID	Latitude	Longitude	Ellipsoid (meters)
1001-91	46° 11' 48.84426"	-118° 58' 46.56810"	99.263
RZ1298	46° 31' 12.75341"	-117° 34' 11.56569"	634.467
RZ1704	46° 39' 18.40564"	-117° 34' 25.98768"	593.638
SA1759	46° 05' 04.14324"	-118° 54' 34.51824"	90.576
TUC_01	46° 30' 10.94831"	-117° 58' 24.57279"	270.84
TUC_02	46° 28' 04.69851"	-117° 54' 23.95748"	319.686
TUC_03	46° 26' 32.32468"	-117° 44' 49.01782"	439.099
TUC_07	46° 15' 41.37590"	-117° 40' 04.54551"	772.284
WA3CO_01	46° 12' 33.36158"	-117° 34' 50.57615"	1676.905
WA3CO_02	46° 10' 00.36979"	-117° 31' 37.16838"	1787.194
WA3CO_03	46° 03' 35.65619"	-117° 48' 01.52231"	1647.104
WA3CO_04	46° 07' 19.40445"	-117° 50' 34.14169"	1653.937
WA3CO_05	46° 16' 59.49959"	-117° 46' 59.33029"	1113.001
WA3CO_06	46° 29' 02.16256"	-118° 20' 45.30227"	417.450
WA3CO_07	46° 21' 44.89185"	-118° 40' 30.63394"	213.521
WALLA_04	46° 01' 27.74937"	-118° 20' 47.90277"	245.491
WALLA_05	46° 06' 07.37924"	-118° 15' 11.02924"	365.994
RTK_ONLY	46° 21' 54.14701"	-117° 34' 11.78227"	1117.851

Table 5: Federal Geographic Data Committee monument rating for network accuracy

Direction	Rating
1.96 * St Dev $_{NE}$:	0.020 m
1.96 * St Dev $_{z}$:	0.020 m

Table 6: Permanent base stations utilized for the Washington 3 Counties acquisition. Coordinates are on the NAD83 (CORS96) datum, epoch 2002.00

CORS ID	Owner	Latitude	Longitude	Ellipsoid (meters)
ANAT	WSRN	46° 07' 58.29490"	-117° 08' 07.48062"	1087.775
CCPW	WSRN	46° 19' 16.31812"	-117° 58' 42.88324"	497.798
IDLW	LEICA	46° 24' 32.13916"	-117° 01' 34.17326"	249.723
KENI	WSRN	46° 11' 52.36533"	-119° 09' 31.01593"	146.542
KLTS	WSRN	46° 38' 35.52937"	-118° 33' 29.34766"	257.666
LWST	WSRN	46° 22' 23.42488"	-117° 00' 08.24688"	427.599
ORPE	LEICA	45° 40' 15.33064"	-118° 51' 00.63585"	312.565
PLMN	WSRN	46° 44' 02.13454"	-117° 11' 35.11470"	743.434
WALA	WSRN	46° 05' 29.41968"	-118° 15' 29.25418"	369.238
WAPA	LEICA	46° 14' 56.67995"	-119° 04' 49.15362"	6.866
WAWL	LEICA	46° 04' 54.53775"	-118° 16' 55.93229"	67.674

Ground Survey Points (GSPs)

Ground survey points were collected using real time kinematic (RTK), post-processed kinematic (PPK), and fast-static (FS) survey techniques. For RTK surveys, a base station or Real-Time Network (RTN) would broadcast kinematic corrections to roving GNSS receivers; for FS and PPK surveys, these corrections must be post-processed. All GSP measurements were made during periods with a Position Dilution of Precision (PDOP) of ≤ 3.0 with at least six satellites in view of the stationary and roving receivers. When collecting RTK and PPK data, the rover records data while stationary for five seconds, then calculates the pseudorange position using at least three one-second epochs. FS surveys record observations for up to fifteen minutes on each GSP in order to support longer baselines for post-processing. Relative errors for any GSP position must be less than 1.5 cm horizontal and 2.0 cm vertical in order to be accepted. See Table 7 for Trimble unit specifications.

GSPs were collected in areas where good satellite visibility was achieved on paved roads and other hard surfaces such as gravel or packed dirt roads. GSP measurements were not taken on highly reflective surfaces such as center line stripes or lane markings on roads due to the increased noise seen in the laser returns over these surfaces. GSPs were collected within as many flightlines as possible; however, the distribution of GSPs depended on ground access constraints and monument locations and may not be equitably distributed throughout the study area (Figure 2).

Table 7: Trimble equipment identification

Receiver Model	Antenna	OPUS Antenna ID	Use
Trimble R6	Integrated GNSS Antenna R6	TRM_R6	Rover
Trimble R7 GNSS	Zephyr GNSS Geodetic Model 2 RoHS	TRM57971.00	Static, Rover
Trimble R8	Integrated Antenna R8 Model 2	TRM_R8_GNSS	Rover
Trimble R10	Integrated Antenna R10	TRMR10	Rover

Land Cover Class

In addition to ground survey points, land cover class check points were collected throughout the study area to evaluate vertical accuracy. Vertical accuracy statistics were calculated for all land cover types to assess confidence in the LiDAR derived ground models across land cover classes (Table 8, see LiDAR Accuracy Assessments, page 23).

Table 8: Land Cover Types and Descriptions

Land cover type	Land cover code	Example	Description	Accuracy Assessment Type
Bare Earth	BARE		Areas of bare earth surface	NVA
Urban	URBAN		Areas of urban development	NVA

Land cover type	Land cover code	Example	Description	Accuracy Assessment Type
Tall Grass	TALL_GRASS		Herbaceous grasslands in advanced stages of growth	VVA
Shrubland	SHRUB		Herbaceous shrublands	VVA
Mixed Forest	FOREST		Forested areas comprised of both deciduous and coniferous species	VVA

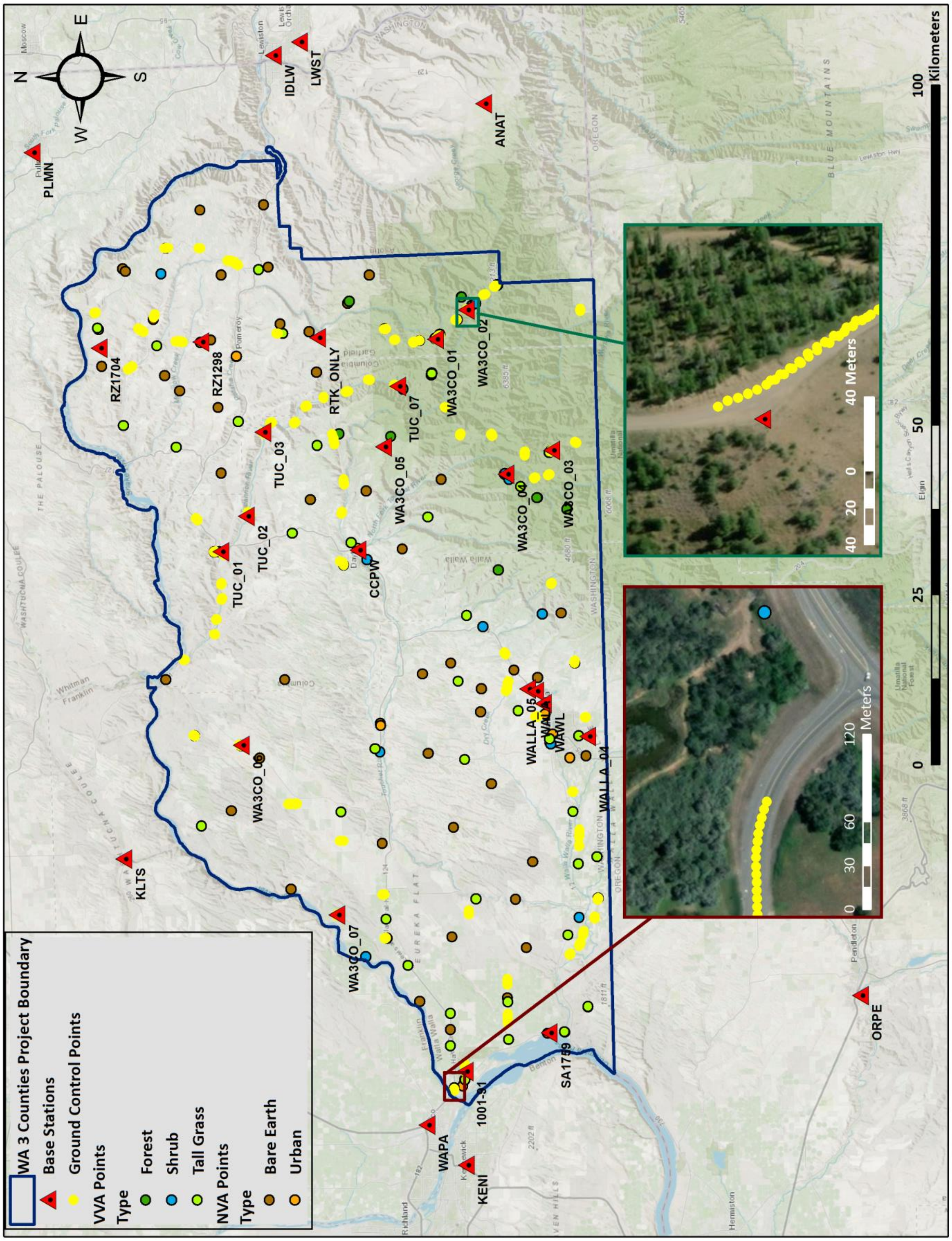

Figure 2: Ground survey location map

This 10 foot LiDAR cross section shows a view of a house and vegetation on the bank of the Snake River in the Washington 3 Counties AOI, colored by point classification.

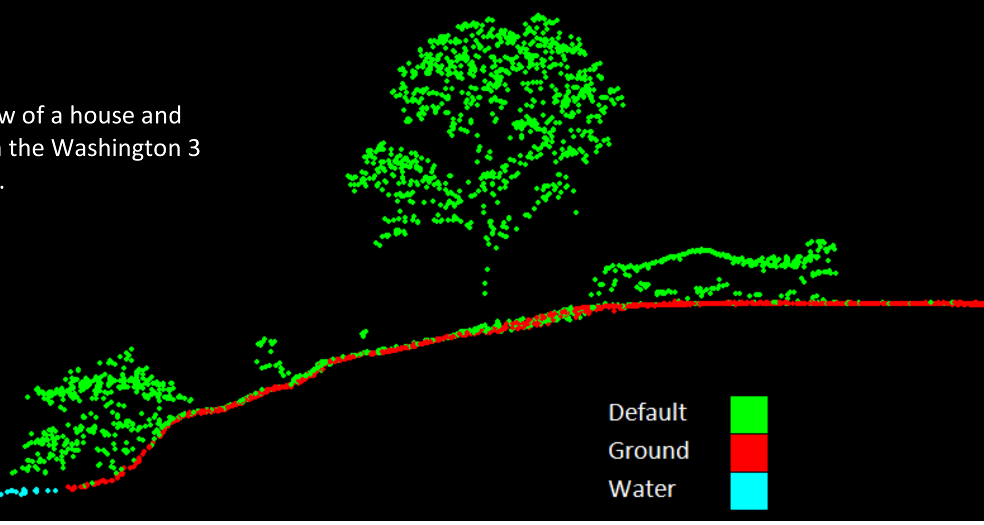

LiDAR Data

Upon completion of data acquisition, QSI processing staff initiated a suite of automated and manual techniques to process the data into the requested deliverables. Processing tasks included GPS control computations, smoothed best estimate trajectory (SBET) calculations, kinematic corrections, calculation of laser point position, sensor and data calibration for optimal relative and absolute accuracy, and LiDAR point classification (Table 9). Processing methodologies were tailored for the landscape. Brief descriptions of these tasks are shown in Table 10.

Table 9: ASPRS LAS classification standards applied to the Washington 3 Counties dataset

Classification Number	Classification Name	Classification Description
1	Default/Unclassified	Laser returns that are not included in the ground class, composed of vegetation and anthropogenic features
1-O	Overlap/Edge Clip	Flightline edge clip that is withheld because it does not contribute to the utility of the dataset, but may be maintained as a reference
2	Ground	Laser returns that are determined to be ground using automated and manual cleaning algorithms
7	Noise	Laser returns that are often associated with birds, scattering from reflective surfaces, or artificial points below the ground surface
9	Water	Laser returns that are determined to be water using automated and manual cleaning algorithms
10	Ignored Ground	Ground points proximate to water's edge breaklines; ignored for correct model creation
17	Bridge	Bridge decks
21	Temporal Snow	Areas which have possible snow coverage, identified during LiDAR processing

Temporal Snow Classification

While processing the Washington 3 Counties LiDAR dataset, QSI production staff members made note of areas within the project site that appeared to have, or may have had, snow on the ground, which would affect the laser's ability to penetrate to the ground surface. These areas were identified by manually drawing temporal snow polygons during processing to identify and reclassify areas that may contain snow, which could cause temporal differences in the ground surface of the LiDAR point cloud. The majority of the areas within the snow polygon were captured by two missions, one having little or no snow on the ground at the time. Thus these areas should be considered to be ground classified, with the potential use limitation taken into account for any analysis purposes (Table 9).

Table 10: LiDAR processing workflow

LiDAR Processing Step	Software Used
Resolve kinematic corrections for aircraft position data using kinematic aircraft GPS and static ground GPS data. Develop a smoothed best estimate of trajectory (SBET) file that blends post-processed aircraft position with sensor head position and attitude recorded throughout the survey.	Waypoint Inertial Explorer v.8.7
Calculate laser point position by associating SBET position to each laser point return time, scan angle, intensity, etc. Create raw laser point cloud data for the entire survey in *.las (ASPRS v. 1.4) format. Convert data to orthometric elevations by applying a geoid correction.	Waypoint Inertial Explorer v.8.7 Leica Cloudpro v. 1.2.2
Import raw laser points into manageable blocks (less than 500 MB) to perform manual relative accuracy calibration and filter erroneous points. Classify ground points for individual flight lines.	TerraScan v.18
Using ground classified points per each flight line, test the relative accuracy. Perform automated line-to-line calibrations for system attitude parameters (pitch, roll, heading), mirror flex (scale) and GPS/IMU drift. Calculate calibrations on ground classified points from paired flight lines and apply results to all points in a flight line. Use every flight line for relative accuracy calibration.	TerraMatch v.18
Classify resulting data to ground and other client designated ASPRS classifications (Table 9). Assess statistical absolute accuracy via direct comparisons of ground classified points to ground control survey data.	TerraScan v.18 TerraModeler v.18
Generate bare earth models as triangulated surfaces. Generate highest hit models as a surface expression of all classified points. Export all surface models as ESRI GRIDs at a 3.0 foot pixel resolution.	TerraScan v.18 TerraModeler v.18 ArcMap v. 10.3.1
Correct intensity values for variability and export intensity images as GeoTIFFs at a 3 foot pixel resolution.	Las Monkey 2.3.4 (QSI proprietary) LAS Product Creator 3.0 (QSI proprietary) ArcMap v. 10.3.1

Feature Extraction

Hydro-flattening and Water's Edge Breaklines

The bounding river on the east and north sides of the Washington 3 Counties site and other water bodies within the project area were flattened to a consistent water level. Bodies of water that were flattened include lakes and other closed water bodies with a surface area greater than 2 acres and all streams and rivers that are nominally wider than 100 feet. Islands within water bodies with area greater than 1 acre were not hydroflattened, with select smaller islands and features remaining as feasible. The hydroflattening process eliminates artifacts in the digital terrain model caused by both increased variability in ranges or dropouts in laser returns due to the low reflectivity of water.

Hydroflattening of closed water bodies was performed through a combination of automated and manual detection and adjustment techniques designed to identify water boundaries and water levels. Boundary polygons were developed using an algorithm which weights LiDAR-derived slopes, intensities, and return densities to detect the water's edge. The water edges were then manually reviewed and edited as necessary.

Once polygons were developed the initial ground classified points falling within water polygons were reclassified as water points to omit them from the final ground model. Elevations were then obtained from the filtered LiDAR returns to create the final breaklines. Lakes were assigned a consistent elevation for an entire polygon while rivers were assigned consistent elevations on opposing banks and smoothed to ensure downstream flow through the entire river channel.

Water boundary breaklines were then incorporated into the hydro-flattened DEM by enforcing triangle edges (adjacent to the breakline) to the elevation values of the breakline. This implementation corrected interpolation along the hard edge.

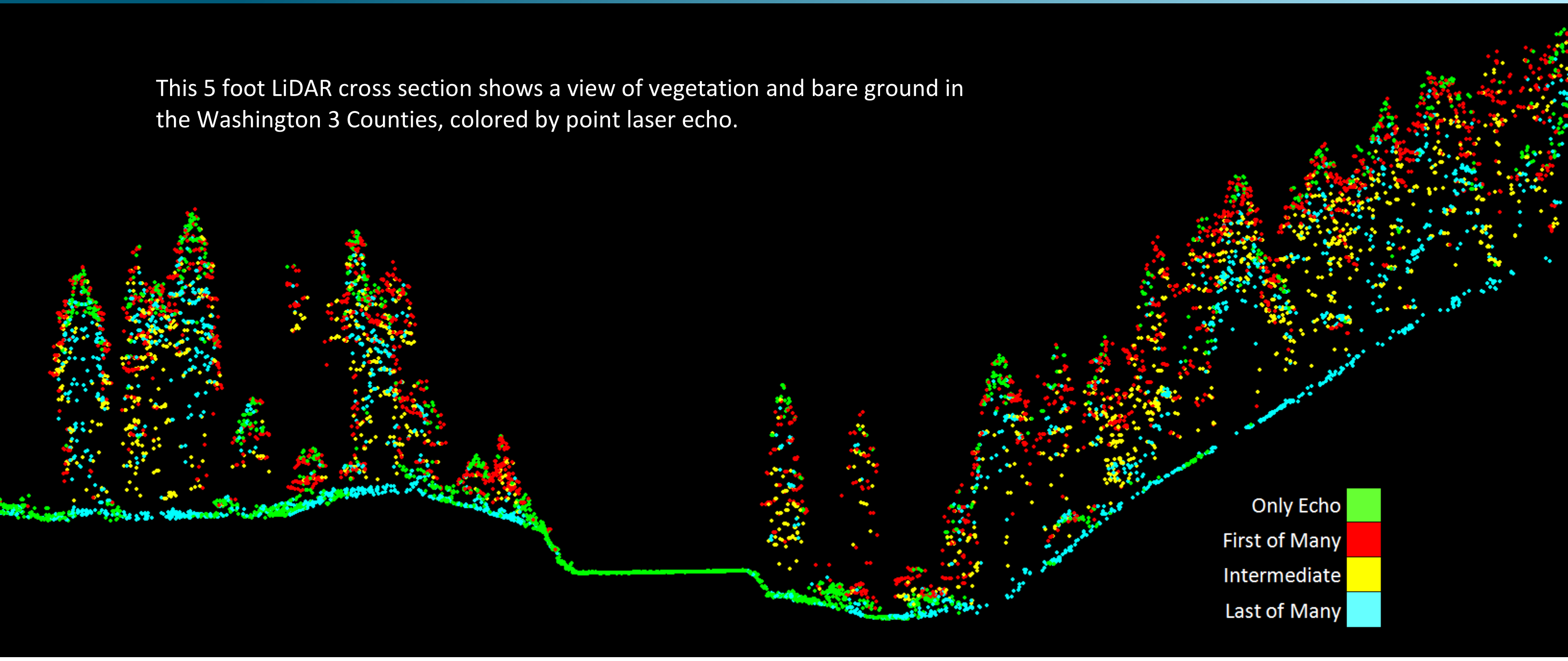

LiDAR Density

The acquisition parameters were designed to acquire an average first-return density of ≥8 points/m^2 (0.74 points/ft^2) for QL1 AOIs and ≥2 points/m^2 (0.19 points/ft^2) for QL2 AOIs. First return density describes the density of pulses emitted from the laser that return at least one echo to the system. Multiple returns from a single pulse were not considered in first return density analysis. Some types of surfaces (e.g., breaks in terrain, water and steep slopes) may have returned fewer pulses than originally emitted by the laser. First returns typically reflect off the highest feature on the landscape within the footprint of the pulse. In forested or urban areas the highest feature could be a tree, building or power line, while in areas of unobstructed ground, the first return will be the only echo and represents the bare earth surface.

The density of ground-classified LiDAR returns was also analyzed for this project. Terrain character, land cover, and ground surface reflectivity all influenced the density of ground surface returns. In vegetated areas, fewer pulses may penetrate the canopy, resulting in lower ground density.

The average first-return density of LiDAR data for the QL1 portion of the Washington 3 Counties project was 1.16 points/ft^2 (12.54 points/m^2) while the average ground classified density was 0.62 points/ft^2 (6.63 points/m^2). The average first-return density of LiDAR data for the QL2 portion of the Washington 3 Counties project was 0.54 points/ft^2 (5.82 points/m^2) while the average ground classified density was 0.32 points/ft^2 (3.48 points/m^2) The statistical and spatial distributions of first return densities and classified ground return densities per 100 m x 100 m cell are portrayed in Figure 3 through Figure 8.

Table 11: Average LiDAR point densities

Classification	Point Density		
	QL1 AOI	**QL2 AOI**	**Combined**
First-Return	1.16 points/ft^2 12.54 points/m^2	0.54 points/ft^2 5.82 points/m^2	0.86 points/ft^2 9.29 points/m^2
Ground Classified	0.62 points/ft^2 6.63 points/m^2	0.32 points/ft^2 3.48 points/m^2	0.48 points/ft^2 5.12 points/m^2

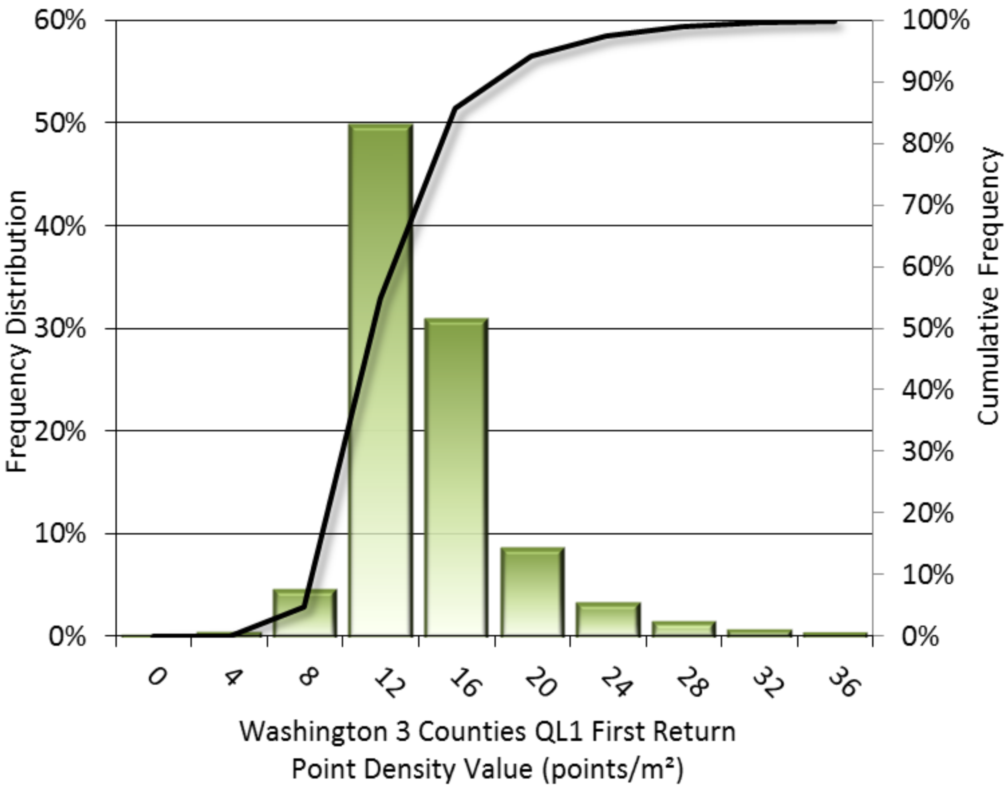

Figure 3: Frequency distribution of first return point density values per 100 x 100 m cell

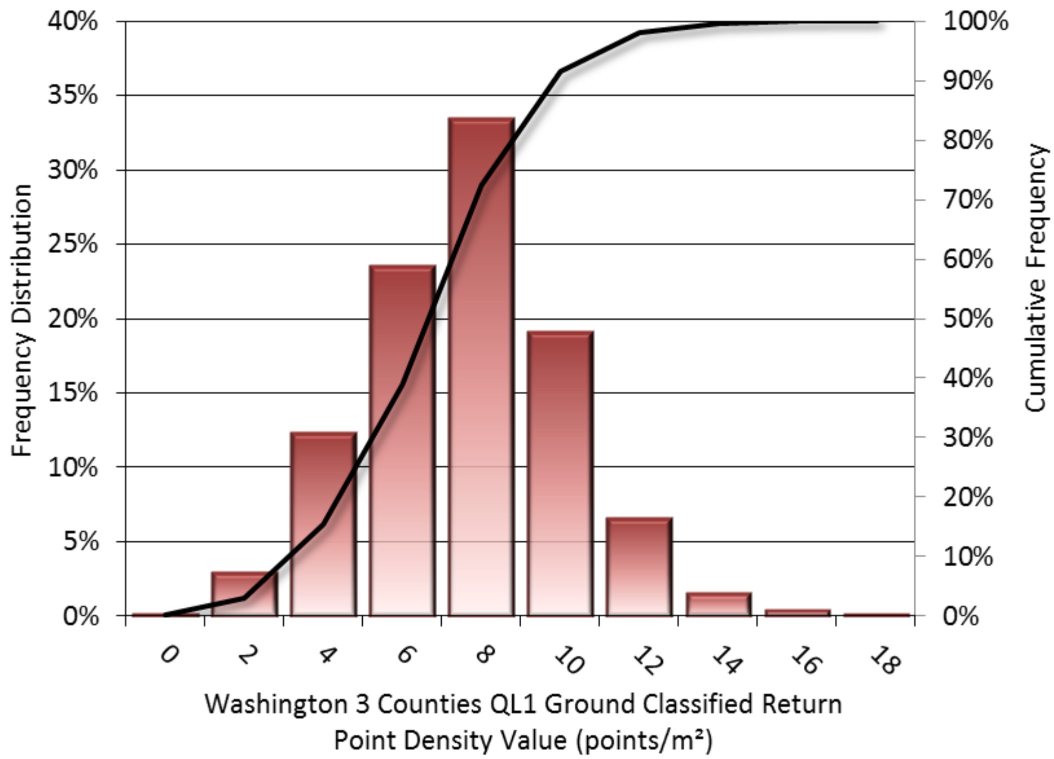

Figure 4: Frequency distribution of ground-classified return point density values per 100 x 100 m cell

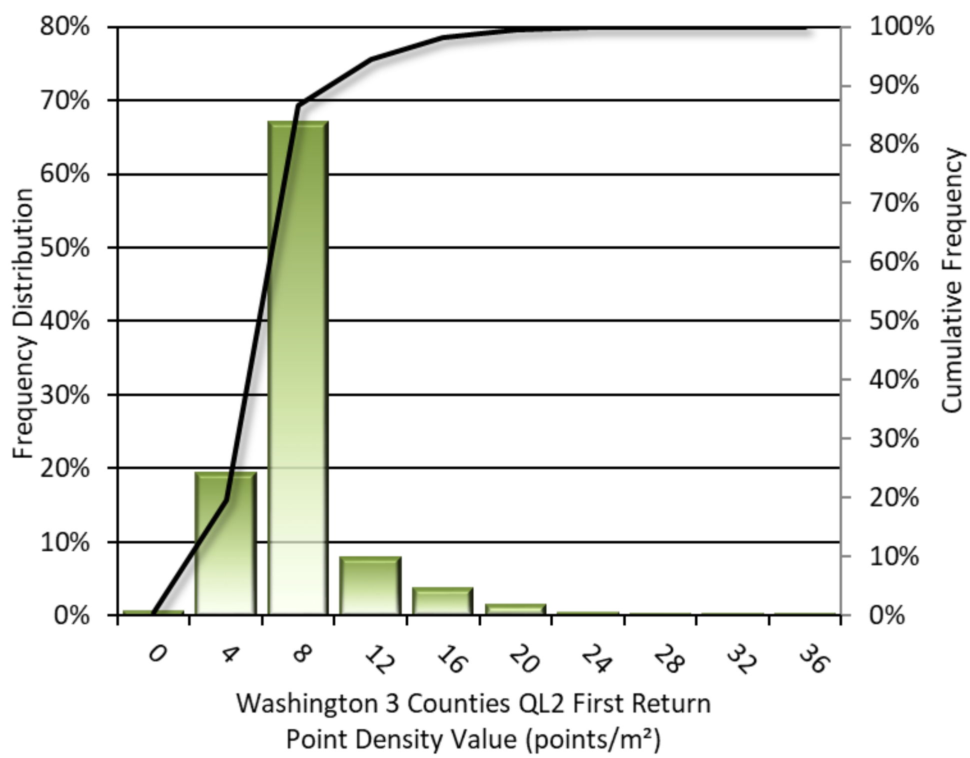

Figure 5: Frequency distribution of first return point density values per 100 x 100 m cell

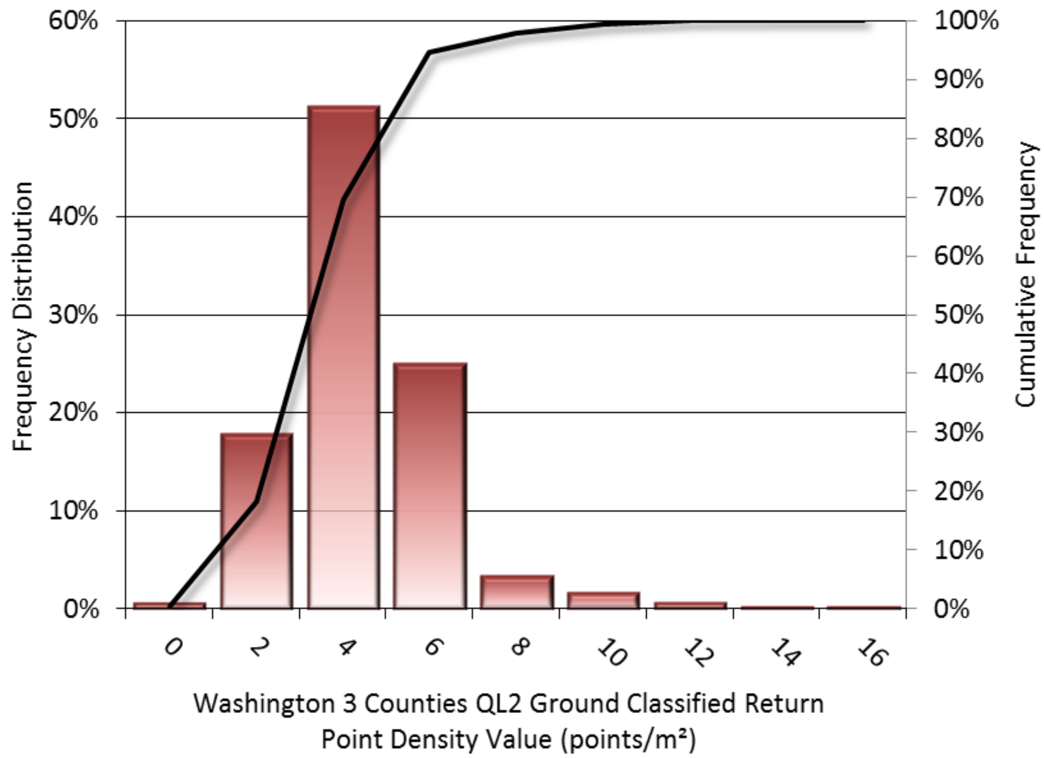

Figure 6: Frequency distribution of ground-classified return point density values per 100 x 100 m cell

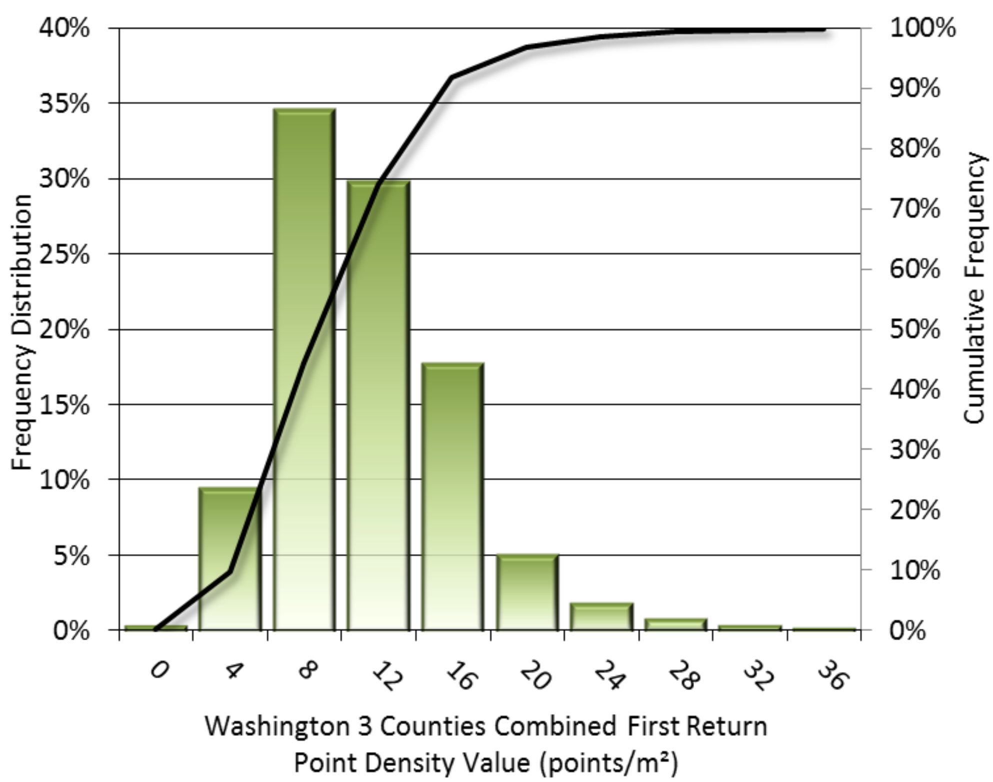

Figure 7: Frequency distribution of first return point density values per 100 x 100 m cell

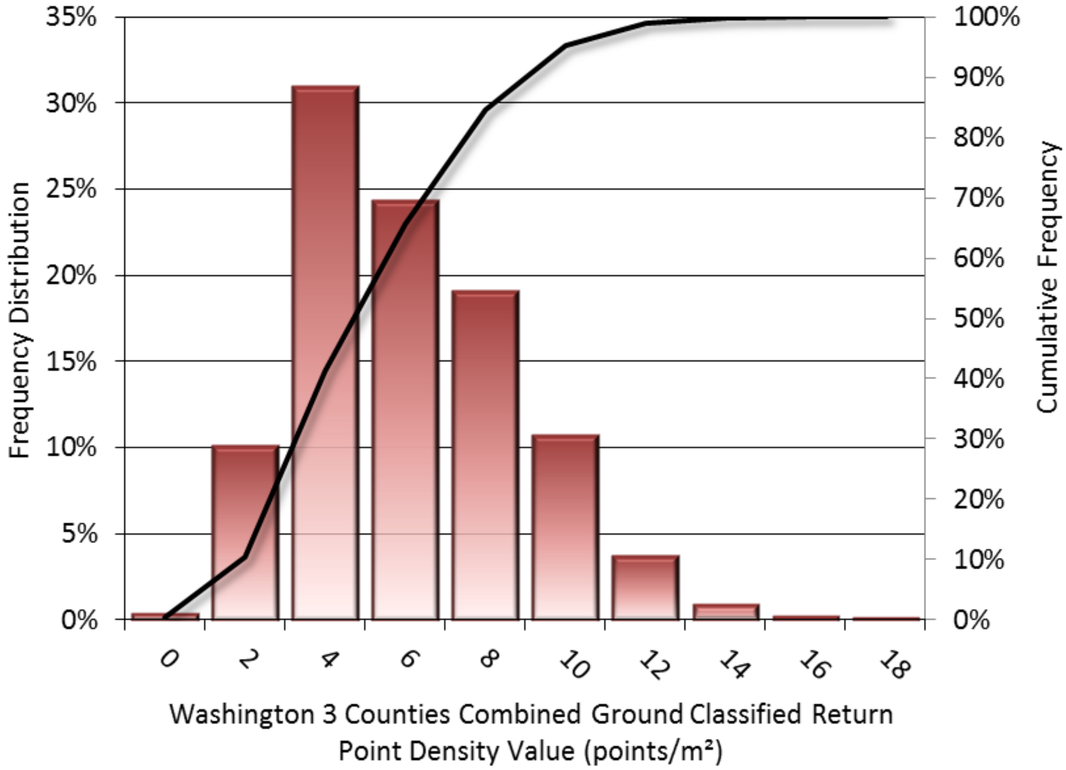

Figure 8: Frequency distribution of ground-classified return point density values per 100 x 100 m cell

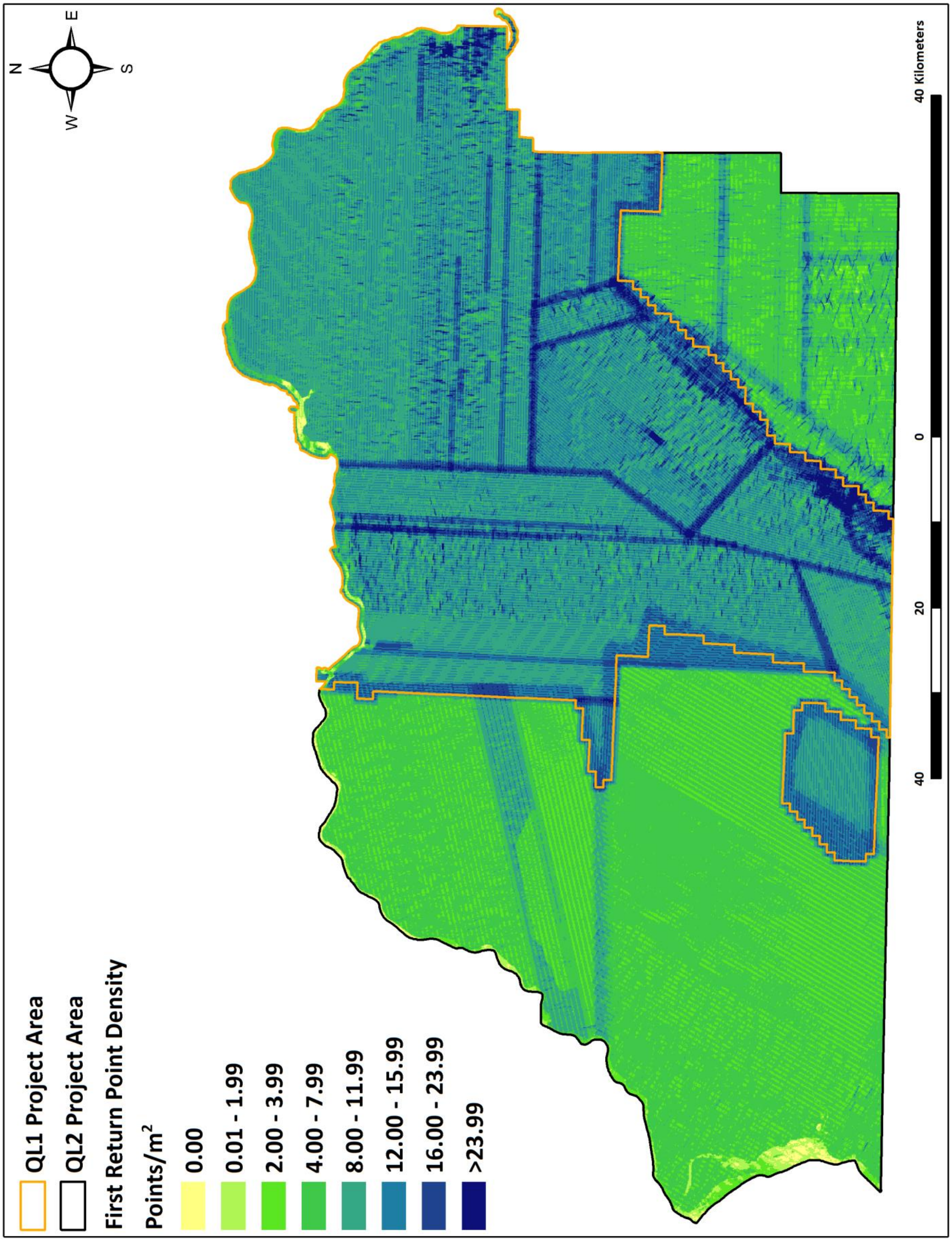

Figure 9: First return point density map for the Washington 3 Counties site (100 m x 100 m cells)

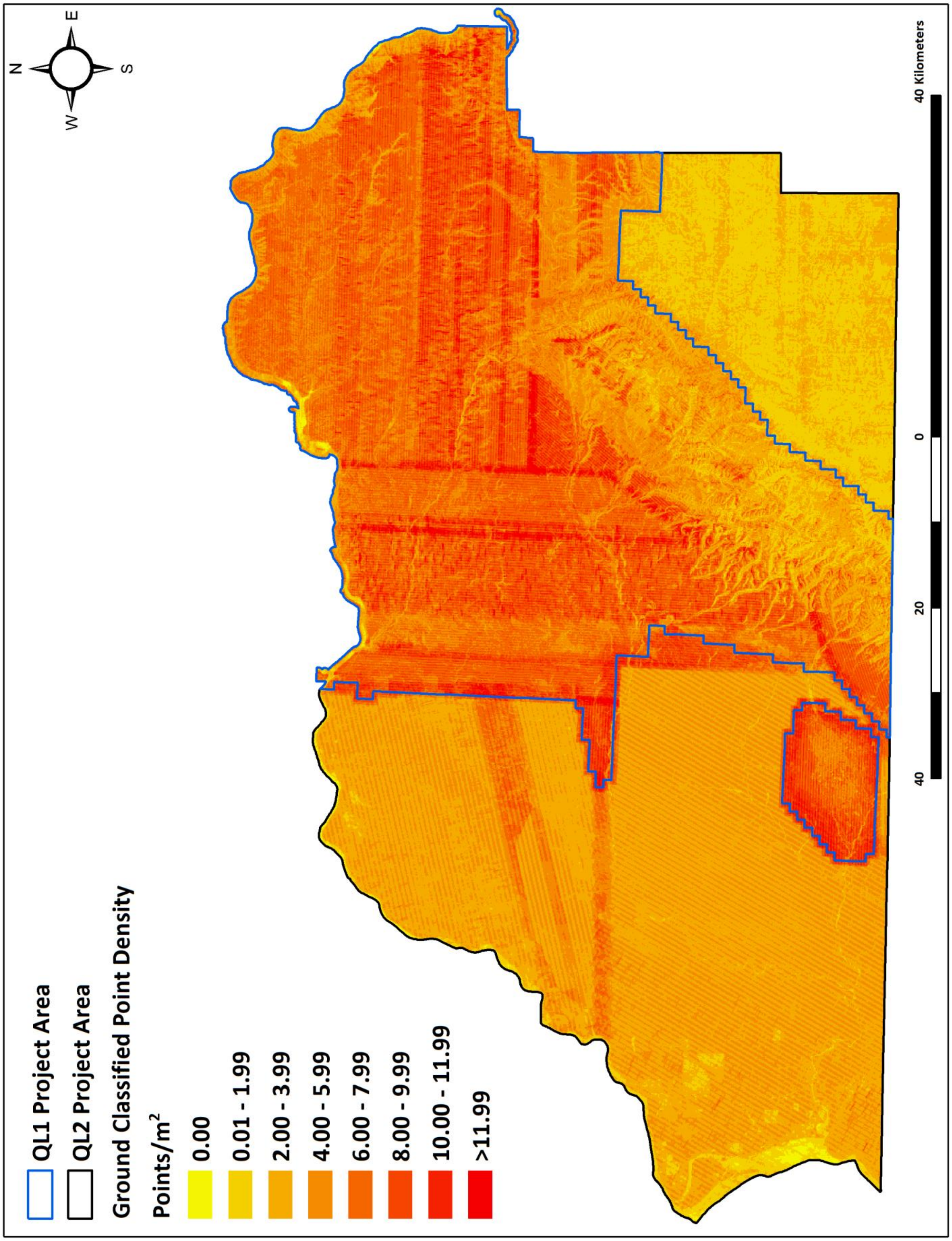

Figure 10: Ground point density map for the Washington 3 Counties site (100 m x 100 m cells)

LiDAR Accuracy Assessments

The accuracy of the LiDAR data collection can be described in terms of absolute accuracy (the consistency of the data with external data sources) and relative accuracy (the consistency of the dataset with itself). See Appendix A for further information on sources of error and operational measures used to improve relative accuracy.

LiDAR Non-Vegetated Vertical Accuracy

Absolute vertical accuracy was assessed using Non-Vegetated Vertical Accuracy (NVA) reporting designed to meet guidelines presented in the FGDC National Standard for Spatial Data Accuracy[3] (NSSDA). NVA compares known ground quality assurance point data collected on open, bare earth surfaces with level slope (<20°) to the triangulated surface generated by the LiDAR points. NVA is a measure of the accuracy of LiDAR point data in open areas where the LiDAR system has a high probability of measuring the ground surface and is evaluated at the 95% confidence interval (1.96 * RMSE), as shown in Table 12.

The mean and standard deviation (sigma σ) of divergence of the ground surface model from quality assurance point coordinates are also considered during accuracy assessment. These statistics assume the error for x, y and z is normally distributed, and therefore the skew and kurtosis of distributions are also considered when evaluating error statistics. For the Washington 3 Counties survey, 85 quality assurance points tested 0.253 feet (0.077 meters) vertical accuracy at 95 percent confidence level as compared to the bare earth DEM (Figure 11), and 0.273 feet (0.083 meters) vertical accuracy at 95 percent confidence level as compared to the unclassified point cloud (Figure 12).

QSI also assessed absolute accuracy using 6,274 supplemental ground control points. Although these points were used in the calibration and post-processing of the LiDAR point cloud, they still provide a good indication of the overall accuracy of the LiDAR dataset, and therefore have been provided in Table 12 and Figure 13.

---

[3] Federal Geographic Data Committee, ASPRS POSITIONAL ACCURACY STANDARDS FOR DIGITAL GEOSPATIAL DATA EDITION 1, Version 1.0, NOVEMBER 2014. http://www.asprs.org/PAD-Division/ASPRS-POSITIONAL-ACCURACY-STANDARDS-FOR-DIGITAL-GEOSPATIAL-DATA.html.

Table 12: Absolute accuracy results

Absolute Vertical Accuracy			
	NVA, as compared to bare earth DEM	NVA, as compared to unclassified LAS	Ground Control Points
Sample	85 points	85 points	6,274 points
95% Confidence (1.96*RMSE)	0.253 ft 0.077 m	0.273 ft 0.083 m	0.229 ft 0.070 m
Average	0.022 ft 0.007 m	0.071 ft 0.022 m	-0.006 ft -0.002 m
Median	0.029 ft 0.009 m	0.062 ft 0.019 m	-0.010 ft -0.003 m
RMSE	0.129 ft 0.039 m	0.139 ft 0.042 m	0.117 ft 0.036 m
Standard Deviation (1σ)	0.128 ft 0.039 m	0.121 ft 0.037 m	0.117 ft 0.036 m

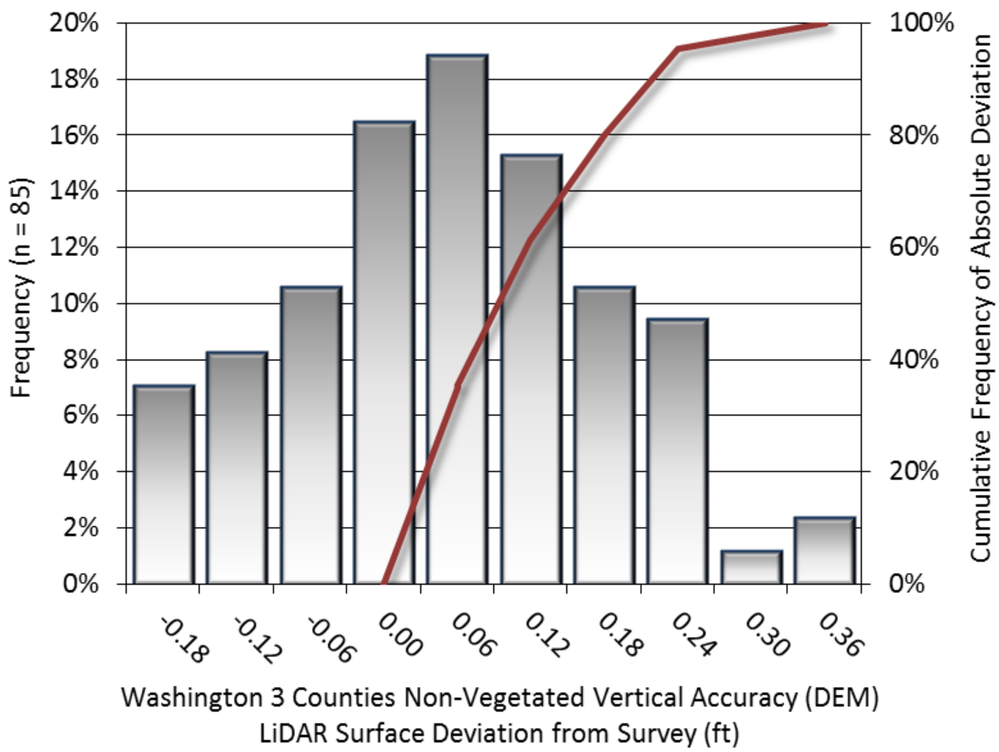

Figure 11: Frequency histogram for LiDAR bare earth DEM deviation from ground check point values (NVA)

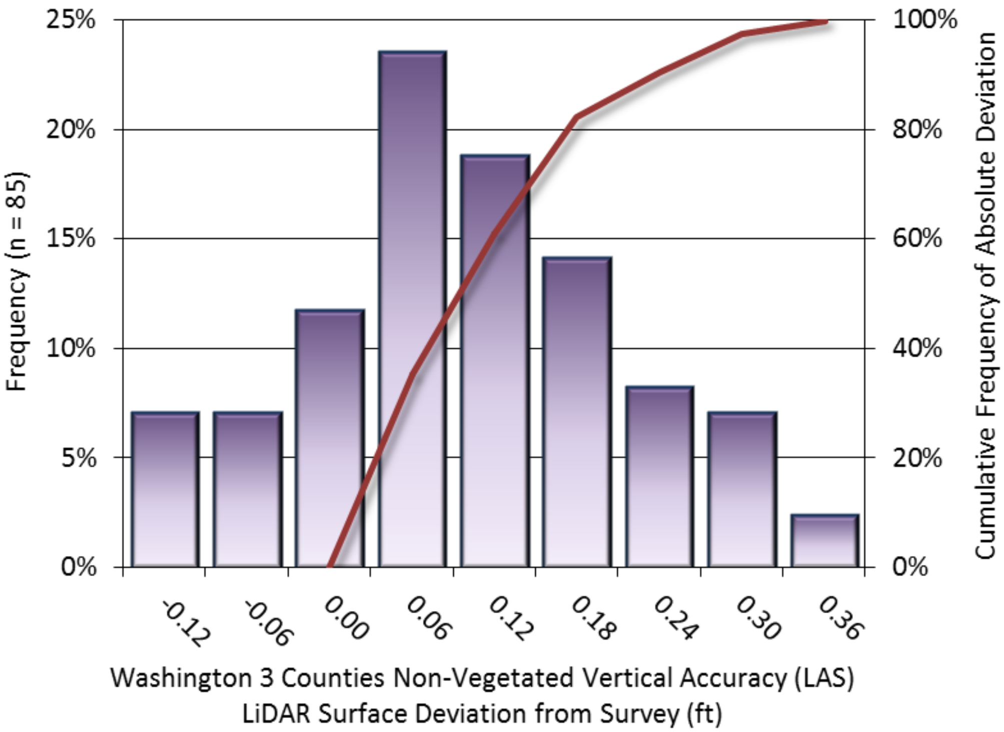

Figure 12: Frequency histogram for LiDAR unclassified LAS surface deviation from ground check point values (NVA)

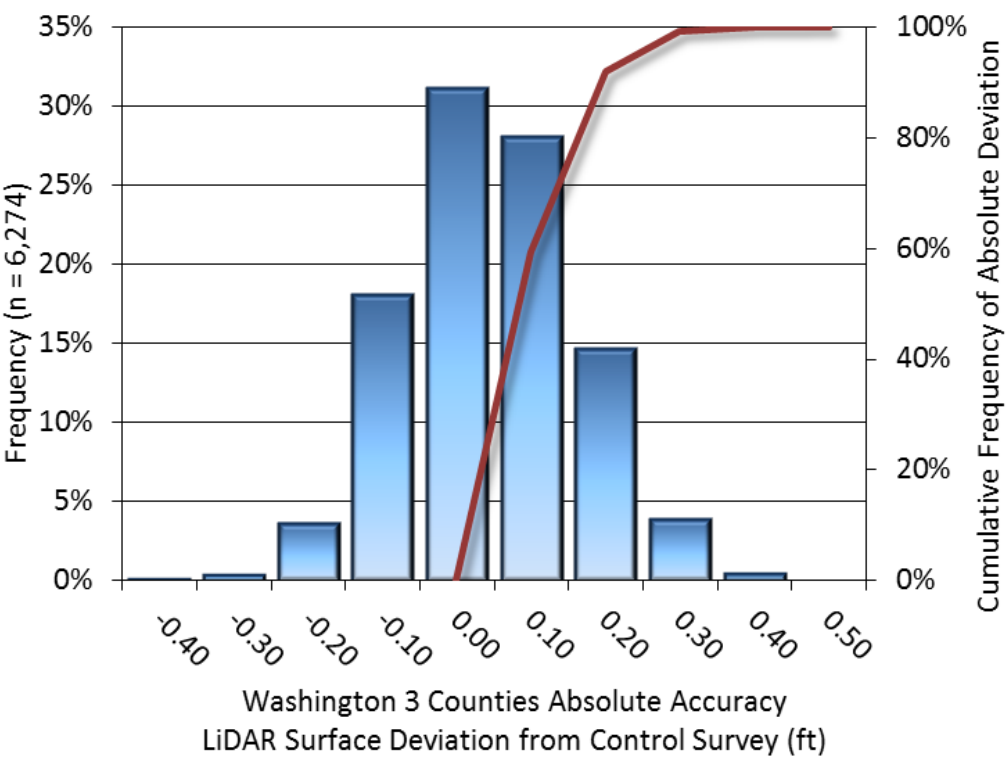

Figure 13: Frequency histogram for LiDAR surface deviation from ground control point values

LiDAR Vegetated Vertical Accuracy

QSI also assessed vertical accuracy using Vegetated Vertical Accuracy (VVA) reporting. VVA compares known ground check point data collected over vegetated surfaces to the triangulated ground surface generated by the ground classified LiDAR points. For the Washington 3 Counties survey, 79 vegetated check points were collected, with resulting vegetated vertical accuracy of 0.675 feet (0.206 meters) as compared to the bare earth DEM, evaluated at the 95th percentile (Table 13, Figure 14).

Table 13: Vegetated vertical accuracy results

Vegetated Vertical Accuracy	
Sample	79 points
95th Percentile	0.675 ft 0.206 m
Average	0.244 ft 0.074 m
Median	0.217 ft 0.066 m
RMSE	0.328 ft 0.100 m
Standard Deviation (1σ)	0.221 ft 0.067 m

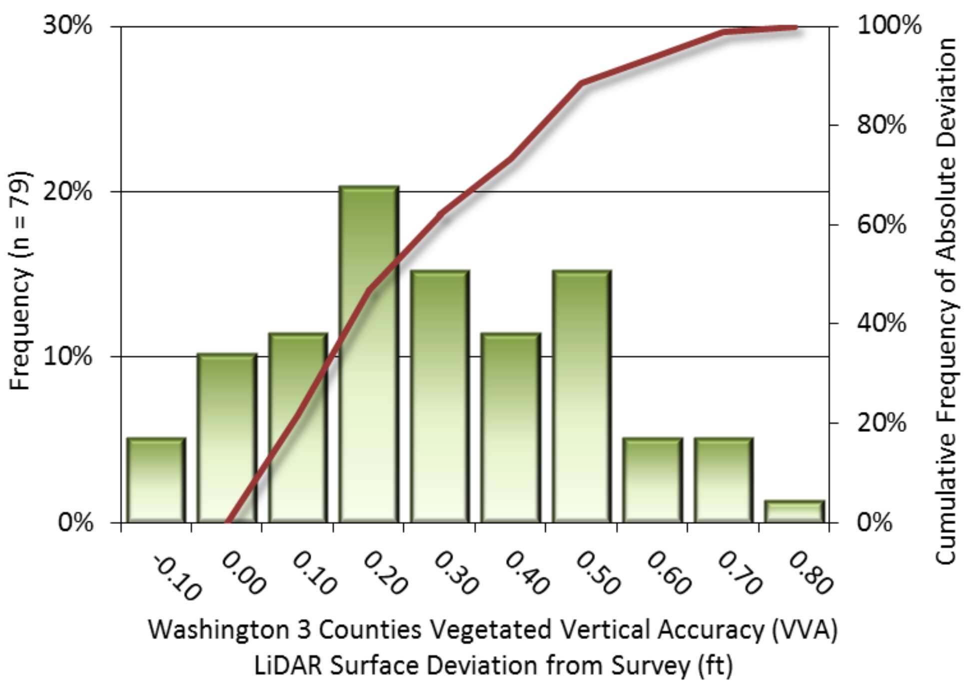

Figure 14: Frequency histogram for LiDAR surface deviation from vegetated check point values (VVA)

LiDAR Relative Vertical Accuracy

Relative vertical accuracy refers to the internal consistency of the data set as a whole: the ability to place an object in the same location given multiple flight lines, GPS conditions, and aircraft attitudes. When the LiDAR system is well calibrated, the swath-to-swath vertical divergence is low (<0.10 meters). The relative vertical accuracy was computed by comparing the ground surface model of each individual flight line with its neighbors in overlapping regions. The average (mean) line to line relative vertical accuracy for the Washington 3 Counties LiDAR project was 0.105 feet (0.032 meters) (Table 14, Figure 15).

Table 14: Relative accuracy results

Relative Accuracy	
Sample	910 surfaces
Average	0.105 ft 0.032 m
Median	0.102 ft 0.031 m
RMSE	0.153 ft 0.047 m
Standard Deviation (1σ)	0.070 ft 0.021 m
1.96σ	0.138 ft 0.042 m

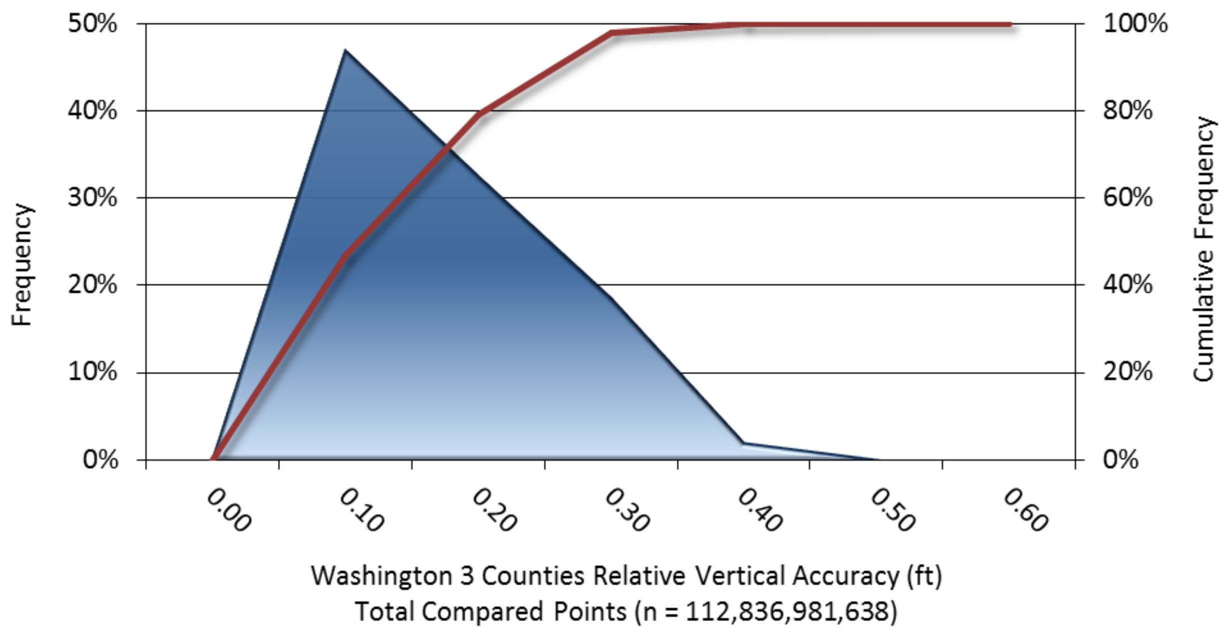

Figure 15: Frequency plot for relative vertical accuracy between flight lines

CERTIFICATIONS

Quantum Spatial, Inc. provided LiDAR services for the Washington 3 Counties project as described in this report.

I, Tucker Selko, have reviewed the attached report for completeness and hereby state that it is a complete and accurate report of this project.

Tucker Selko
Tucker Selko (Jan 31, 2019) Jan 31, 2019

Tucker Selko
Project Manager
Quantum Spatial, Inc.

I, Evon P. Silvia, PLS, being duly registered as a Professional Land Surveyor in and by the state of Washington, hereby certify that the methodologies, static GNSS occupations used during airborne flights, and ground survey point collection were performed using commonly accepted Standard Practices. Field work conducted for this report was conducted between October 1st, 2017 and May 4th, 2018.

Accuracy statistics shown in the Accuracy Section of this Report have been reviewed by me and found to meet the "National Standard for Spatial Data Accuracy".

Evon P. Silvia Jan 31, 2019

Evon P. Silvia, PLS
Quantum Spatial, Inc.
Corvallis, OR 97330

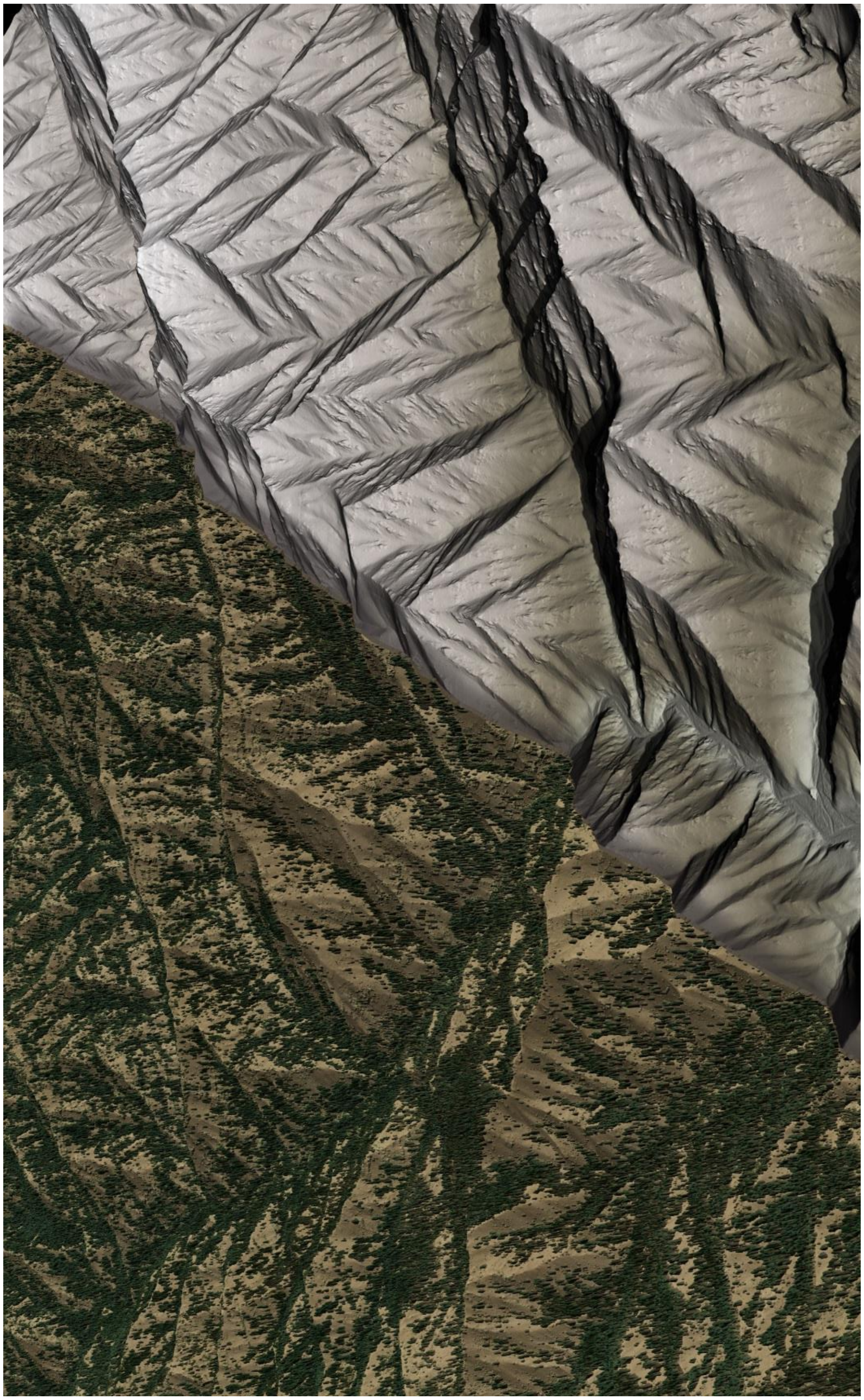

Figure 16: This image shows the intersection of Crooked Creek and Melton Creek in the Washington 3 Counties AOI. The image was created from the LiDAR highest hit model on the left and the LiDAR bare earth model on the right.

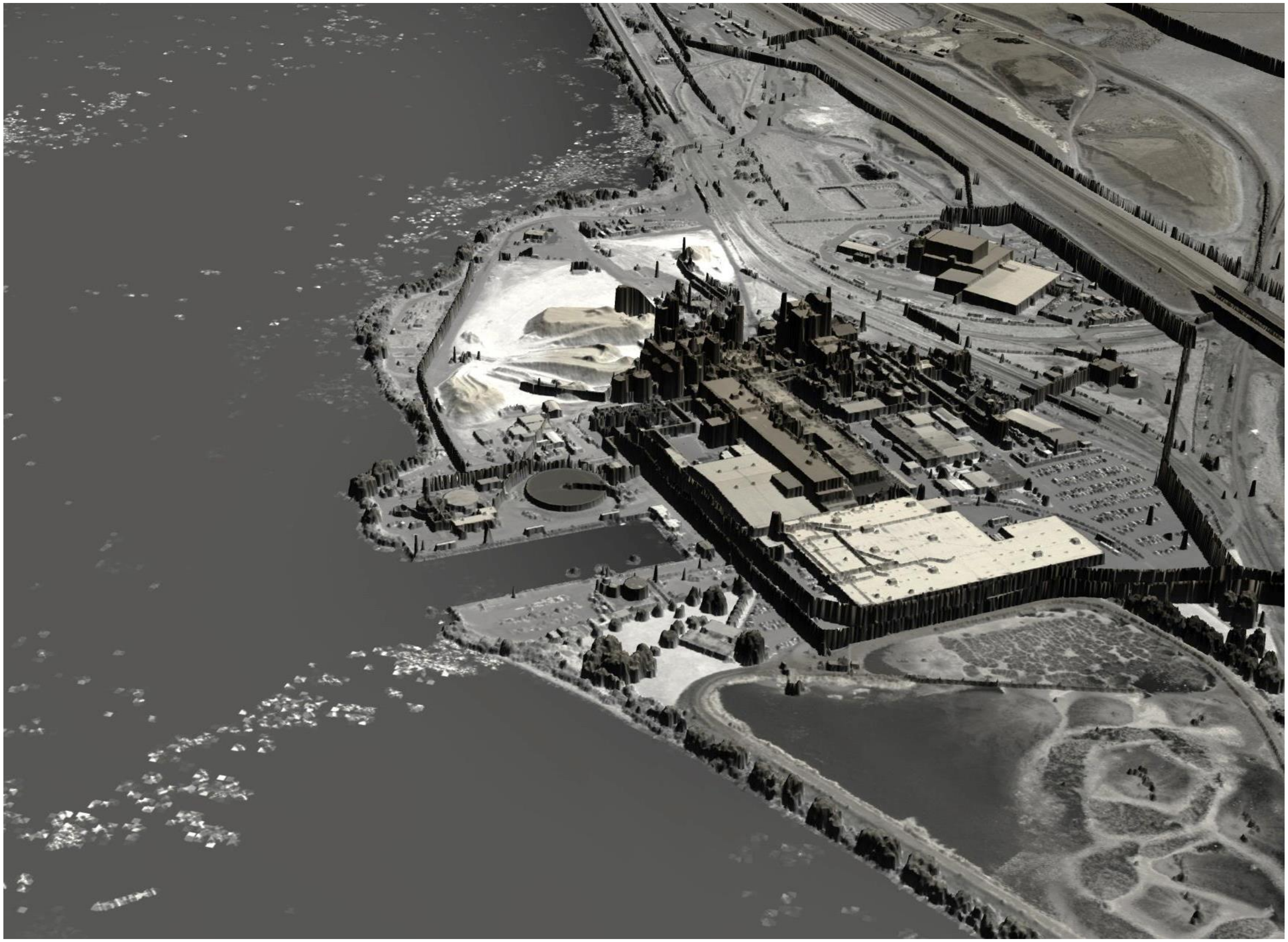

Figure 17: This image shows the Specialty Mineral, Inc. factory on the banks of the Snake River. The image was created from the LiDAR highest hit model and colored by elevation.

GLOSSARY

1-sigma (σ) Absolute Deviation: Value for which the data are within one standard deviation (approximately 68th percentile) of a normally distributed data set.

1.96 * RMSE Absolute Deviation: Value for which the data are within two standard deviations (approximately 95th percentile) of a normally distributed data set, based on the FGDC standards for Non-vegetated Vertical Accuracy (NVA) reporting.

Accuracy: The statistical comparison between known (surveyed) points and laser points. Typically measured as the standard deviation (sigma σ) and root mean square error (RMSE).

> **Absolute Accuracy:** The vertical accuracy of LiDAR data is described as the mean and standard deviation (sigma σ) of divergence of LiDAR point coordinates from ground survey point coordinates. To provide a sense of the model predictive power of the dataset, the root mean square error (RMSE) for vertical accuracy is also provided. These statistics assume the error distributions for x, y and z are normally distributed, and thus we also consider the skew and kurtosis of distributions when evaluating error statistics.
>
> **Relative Accuracy:** Relative accuracy refers to the internal consistency of the data set; i.e., the ability to place a laser point in the same location over multiple flight lines, GPS conditions and aircraft attitudes. Affected by system attitude offsets, scale and GPS/IMU drift, internal consistency is measured as the divergence between points from different flight lines within an overlapping area. Divergence is most apparent when flight lines are opposing. When the LiDAR system is well calibrated, the line-to-line divergence is low (<10 cm).
>
> **Root Mean Square Error (RMSE):** A statistic used to approximate the difference between real-world points and the LiDAR points. It is calculated by squaring all the values, then taking the average of the squares and taking the square root of the average.

Data Density: A common measure of LiDAR resolution, measured as points per square meter.

Digital Elevation Model (DEM): File or database made from surveyed points, containing elevation points over a contiguous area. Digital terrain models (DTM) and digital surface models (DSM) are types of DEMs. DTMs consist solely of the bare earth surface (ground points), while DSMs include information about all surfaces, including vegetation and man-made structures.

Intensity Values: The peak power ratio of the laser return to the emitted laser, calculated as a function of surface reflectivity.

Nadir: A single point or locus of points on the surface of the earth directly below a sensor as it progresses along its flight line.

Overlap: The area shared between flight lines, typically measured in percent. 100% overlap is essential to ensure complete coverage and reduce laser shadows.

Pulse Rate (PR): The rate at which laser pulses are emitted from the sensor; typically measured in thousands of pulses per second (kHz).

Pulse Returns: For every laser pulse emitted, the number of wave forms (i.e., echoes) reflected back to the sensor. Portions of the wave form that return first are the highest element in multi-tiered surfaces such as vegetation. Portions of the wave form that return last are the lowest element in multi-tiered surfaces.

Real-Time Kinematic (RTK) Survey: A type of surveying conducted with a GPS base station deployed over a known monument with a radio connection to a GPS rover. Both the base station and rover receive differential GPS data and the baseline correction is solved between the two. This type of ground survey is accurate to 1.5 cm or less.

Post-Processed Kinematic (PPK) Survey: GPS surveying is conducted with a GPS rover collecting concurrently with a GPS base station set up over a known monument. Differential corrections and precisions for the GNSS baselines are computed and applied after the fact during processing. This type of ground survey is accurate to 1.5 cm or less.

Scan Angle: The angle from nadir to the edge of the scan, measured in degrees. Laser point accuracy typically decreases as scan angles increase.

Native LiDAR Density: The number of pulses emitted by the LiDAR system, commonly expressed as pulses per square meter.

Relative Accuracy Calibration Methodology:

Manual System Calibration: Calibration procedures for each mission require solving geometric relationships that relate measured swath-to-swath deviations to misalignments of system attitude parameters. Corrected scale, pitch, roll and heading offsets were calculated and applied to resolve misalignments. The raw divergence between lines was computed after the manual calibration was completed and reported for each survey area.

Automated Attitude Calibration: All data were tested and calibrated using TerraMatch automated sampling routines. Ground points were classified for each individual flight line and used for line-to-line testing. System misalignment offsets (pitch, roll and heading) and scale were solved for each individual mission and applied to respective mission datasets. The data from each mission were then blended when imported together to form the entire area of interest.

Automated Z Calibration: Ground points per line were used to calculate the vertical divergence between lines caused by vertical GPS drift. Automated Z calibration was the final step employed for relative accuracy calibration.

LiDAR accuracy error sources and solutions:

Type of Error	Source	Post Processing Solution
GPS (Static/Kinematic)	Long Base Lines	None
	Poor Satellite Constellation	None
	Poor Antenna Visibility	Reduce Visibility Mask
Relative Accuracy	Poor System Calibration	Recalibrate IMU and sensor offsets/settings
	Inaccurate System	None
Laser Noise	Poor Laser Timing	None
	Poor Laser Reception	None
	Poor Laser Power	None
	Irregular Laser Shape	None

Operational measures taken to improve relative accuracy:

Low Flight Altitude: Terrain following was employed to maintain a constant above ground level (AGL). Laser horizontal errors are a function of flight altitude above ground (about 1/3000th AGL flight altitude).

Focus Laser Power at narrow beam footprint: A laser return must be received by the system above a power threshold to accurately record a measurement. The strength of the laser return (i.e., intensity) is a function of laser emission power, laser footprint, flight altitude and the reflectivity of the target. While surface reflectivity cannot be controlled, laser power can be increased and low flight altitudes can be maintained.

Reduced Scan Angle: Edge-of-scan data can become inaccurate. The scan angle was reduced to a maximum of $\pm 15^o$/$\pm 20^o$ from nadir, creating a narrow swath width and greatly reducing laser shadows from trees and buildings.

Quality GPS: Flights took place during optimal GPS conditions (e.g., 6 or more satellites and PDOP [Position Dilution of Precision] less than 3.0). Before each flight, the PDOP was determined for the survey day. During all flight times, a dual frequency DGPS base station recording at 1 second epochs was utilized and a maximum baseline length between the aircraft and the control points was less than 13 nm at all times.

Ground Survey: Ground survey point accuracy (<1.5 cm RMSE) occurs during optimal PDOP ranges and targets a minimal baseline distance of 4 miles between GPS rover and base. Robust statistics are, in part, a function of sample size (n) and distribution. Ground survey points are distributed to the extent possible throughout multiple flight lines and across the survey area.

50% Side-Lap (100% Overlap): Overlapping areas are optimized for relative accuracy testing. Laser shadowing is minimized to help increase target acquisition from multiple scan angles. Ideally, with a 50% side-lap, the nadir portion of one flight line coincides with the swath edge portion of overlapping flight lines. A minimum of 50% side-lap with terrain-followed acquisition prevents data gaps.

Opposing Flight Lines: All overlapping flight lines have opposing directions. Pitch, roll and heading errors are amplified by a factor of two relative to the adjacent flight line(s), making misalignments easier to detect and resolve.